Applied Acoustics 241 (2026) 111033

Contents lists available at ScienceDirect

Applied Acoustics

journal homepage: www.elsevier.com/locate/apacoust

Prediction of coast-by tyre/road noise based on equivalent monopoles synthesised from indoor tests

Samanta Dallasta [a,*], Luca Rapino [a,b], Francesco Ripamonti [a], Simone Baro [b], Roberto Corradi [a]

[a] Politecnico di Milano, Department of Mechanical Engineering, Via La Masa 1, 20156 Milano, Italy
[b] Pirelli Tyre S.p.A., Viale Piero e Alberto Pirelli 25, 20126 Milano, Italy

ARTICLE INFO

Keywords:
Coast-by simulation
Tyre/road noise
Outdoor measurements
Equivalent monopoles
Acoustic transfer functions

ABSTRACT

Tyre/road interaction is the main source of environmental noise pollution, particularly in urban and suburban areas, even at moderate speeds. Its impact is further emphasised by the growing presence of electric vehicles, which significantly reduce the engine's contribution to overall vehicle noise. Indoor testing of tyres is a common practice in the tyre industry during product design stages, as it provides an initial understanding of noise performance. However, outdoor tests are required to assess the noise performance of tyres. For this reason, this study presents a methodology for the prediction of coast-by tyre/road noise based on equivalent sources identified from indoor tests, including the effect of sound reflections due to the vehicle's presence in an outdoor environment. The equivalent monopoles are identified from standalone tyre rolling noise measurements on a test rig equipped with a road replica in a semi-anechoic chamber. To conduct outdoor simulations, acoustic transfer functions are measured on the test track through an omnidirectional acoustic source, with the vehicle positioned on the track. This paper details the experimental setup, data processing, and methodology for carrying out coast-by tyre/road noise simulations based on these equivalent monopoles while accounting for vehicle motion, followed by a comparison with experimental measurements performed using an electric vehicle.

1. Introduction

Environmental noise significantly impacts people's health and well-being. In the 1990s, the EU's Fifth Environment Action Programme (EAP) acknowledged the need for a noise abatement strategy and the tightening of measures on noise emissions [1]. To mitigate its effects, reducing sources of traffic noise is important, as this is the main cause of urban noise pollution [2]. More recently, specific recommendations have been formulated for road traffic noise by the World Health Organization (WHO), which suggests reducing noise levels produced by road traffic below 53 dB for average noise exposure [3].

Regarding vehicle noise sources, tyre/road interaction is the main contributor to road traffic noise at common driving speeds for passenger cars [4,5]. This is increasingly true with the growing market of electric and hybrid vehicles, as well as advances in engine noise reduction. The rising pressure from regulations and the ever-growing consumer expectations contributed to driving tyre manufacturers to develop “quieter” products [6]. In this context, the labelling of tyres was introduced to provide a clear and common classification of tyre performance, which includes external rolling noise class and level [7]. The homologation process for noise levels is based on the test conditions specified in UN ECE Regulation No. 117, which requires the use of a standardized road surface for type approval of tyres. During these tests, the vehicle travels along the noise track, and sound pressure levels are recorded by two microphones positioned on each side of the track according to the coast-by method. In the literature, a notable track-to-track variation was shown, meaning that different ISO tracks can significantly influence the measured external rolling noise values in the range of 4–5 dB [8].

Since the homologation process requires the tyres to be tested in outdoor conditions, a methodology capable of predicting coast-by tests would be useful, as it would reduce the number of tests, saving time and resources, while also ensuring repeatable results. The approach should be able to correctly account for the noise generated by the rolling tyre and include the motion of the vehicle along the test track. However, accurately simulating the noise radiated by a rolling tyre is challenging,

* Corresponding author.
E-mail address: samanta.dallasta@polimi.it (S. Dallasta).

https://doi.org/10.1016/j.apacoust.2025.111033
Received 23 March 2025; Received in revised form 27 July 2025; Accepted 19 August 2025
Available online 28 August 2025

due to the complexity of the mechanisms involved in its generation and amplification [5,9–13].

Different approaches have been proposed in the literature for the prediction of coast-by and pass-by noise of single vehicles. These methodologies can be experimental or numerical, performed either indoors or outdoors, and can involve tests at the complete vehicle level or focused on individual components. Additionally, one or more of these features may be combined within a single predictive framework [14]. Among these, statistical models based on neural networks have been developed, where the predictive model is trained using extensive datasets collected from outdoor tests [15–17]. However, these methods require a large amount of training data and continuous updating, making them less suitable for early design stages. In this context, SPERoN and HyRoNE models are hybrid approaches combining physical and statistical sub-models to predict pass-by noise, using road surface and tyre parameters as inputs to a contact model. Also in this case, large datasets comprising numerous pass-by measurements across different tyre, road surfaces, and speeds are essential to calibrate the regression model coefficients [18,19]. Experimental techniques based on microphone arrays [20–23], instead, aim to predict pass-by noise by measuring tyre noise while the vehicle runs on a chassis dynamometer in an indoor facility. The movement of the vehicle is simulated by switching between the microphones in the array and the final time signal is processed to properly account for the Doppler effect [23]. Finally, an alternative to the current homologation procedure has been presented in [24], where a methodology based on drum tests of a standalone tyre is proposed to determine approved tyre/road noise emission values. In the latter, however, a road surface replica on the drum was not employed.

In this framework, specific modelling techniques have been developed to represent tyre noise through equivalent monopoles or multipole sources. In equivalent sources approaches [25], the primary source is represented by multiple sub-sources, each contributing to the receiver through its source strength multiplied by the corresponding source-receiver transfer functions, allowing for the coast-by noise estimation. These transfer functions may be estimated either numerically [26–30] or experimentally [31,32], taking into account the vehicle geometry. Alternatively, simplified models that consider only the presence of a reflective plane are also found in the literature [33,34].

In the context of equivalent source approaches, the modelling strategies often rely on representations derived from available tyre rolling noise recordings. In [31], a pass-by noise simulation is developed based on the use of noise sources (engine, intake and exhaust system, tyre noise) that are obtained through measurement on indoor test benches and transfer function measured through a loudspeaker. A methodology for the prediction of pass-by noise for automotive vehicles is presented in [27]. The approach is developed in the time domain and uses equivalent sources obtained from indoor near-field recordings on a passenger vehicle. In this case, the source-receiver transfer functions are derived through a numerical simulation that models the vehicle's position at various static points along the track. In [35], instead, a method using the time-domain equivalent source method has been developed to predict pass-by noise of vehicles in a small-scale semi-anechoic chamber. The sound propagation from these sources to the microphones is modelled by half-space Green's function, incorporating ground reflections but without considering possible alterations in sound radiation due to the vehicle's presence.

In this article, a frequency-domain methodology for predicting tyre noise during coast-by tests by means of equivalent monopoles is proposed. The objective of this work is to develop a procedure that employs sources characterized in indoor conditions to predict tyre noise in an outdoor coast-by scenario. The methodology involves identifying equivalent sources from indoor testing of a rolling tyre, based on the deterministic components of the noise, specifically the contribution of the tread pattern and road roughness. These synthesized sources are then used to replicate the coast-by test, incorporating essential phenomena such as the Doppler effect and the time-delay effects of the moving vehicle. In this work, acoustic source-receiver transfer functions are measured through an omnidirectional source both in indoor environment on the test rig and outdoors including the presence of the vehicle. In this way, the measured transfer functions inherently account for the acoustic interactions with both the deformed geometry of the tyre and the vehicle. Finally, the proposed approach includes the comparison with experimental data obtained by coast-by testing at 80 km/h using an electric vehicle.

Compared to previous methodologies, this paper identifies equivalent noise sources directly from the indoor test of a standalone tyre. In fact, drum testing in a semi-anechoic chamber is a common procedure, especially at the prototyping phase. It is important to note, however, that differences between indoor and outdoor test conditions can impact the prediction, and are intrinsic to the use of indoor characterizations for outdoor scenarios. In this study, nominal load, inflation pressure, and road roughness were kept aligned between indoor and outdoor tests. In particular, the drum was equipped with a road surface replica obtained from a mold of the noise track, allowing for road roughness excitation consistent with that of the outdoor conditions.

The structure of this paper is as follows. In Section 2, the description of the methodology used to perform the coast-by prediction taking into account the movement of the vehicle is described. Section 3 presents the outdoor experimental campaign aimed at collecting the coast-by experimental data and the source-receiver transfer functions useful to carry out the predictions. In Section 4, the results of the methodology are discussed and compared with experimental data. Section 5 concludes this study.

2. Coast-by simulation methodology

The developed methodology aims at predicting tyre noise coast-by tests through equivalent monopoles. The proposed approach is shown in the flowchart in Fig. 1. First, an inverse problem is solved: tyre rolling noise ($\boldsymbol{p}_{indoor}$) measured on an indoor test bench, specifically a turret, and experimentally measured acoustic transfer function (H_{indoor}) are used for the synthesis of tyre noise equivalent sources ($\boldsymbol{q}$). At this stage, the equivalent monopoles are fixed and positioned around the tyre. These sources are then applied in the outdoor environment and their motion with the vehicle is simulated for the estimation of coast-by noise. This step can be referred to as a direct problem. The coast-by prediction is performed employing source-receiver transfer functions evaluated experimentally ($H_{outdoor}$). A priori, the acoustic transfer functions may be obtained either by experimental measurement or via numerical simulation. However, in this work, experimental source-receiver transfer functions were chosen to assess the methodology. The result of the coast-by prediction is finally compared with the experimental data obtained from a coast-by noise measurement.

The inverse problem to carry out the synthesis of the equivalent sources was discussed in previous works of the authors [36–39]. The equivalent monopoles for tyre rolling noise were identified based on the deterministic part of tyre rolling noise measurement in the semi-anechoic chamber and experimental acoustic transfer functions H_{indoor}. In particular, the deterministic part of the signal includes the periodic components associated with both the tyre (tread impact and tyre non-uniformity) and the drum rotations (roughness excitation). As a result, each monopole is described as complex spectral components known at multiples of the tyre revolution frequency ($\boldsymbol{q}(\omega_{tread})$) and of the drum revolution frequency ($\boldsymbol{q}(\omega_{road})$). For what concerns the latter, it is important to note that the drum was equipped with a road replica of the surface used in the outdoor coast-by tests. As a first approximation, it is assumed that the use of this road replica on the drum adequately represents the effects of road roughness excitation, which is a random stationary process outdoors. In this way, this approach allows for controlled and repeatable testing while preserving the characteristics of the road texture influencing tyre–road interaction and noise generation.

To carry out the inverse problem, the setup shown in Fig. 2 was

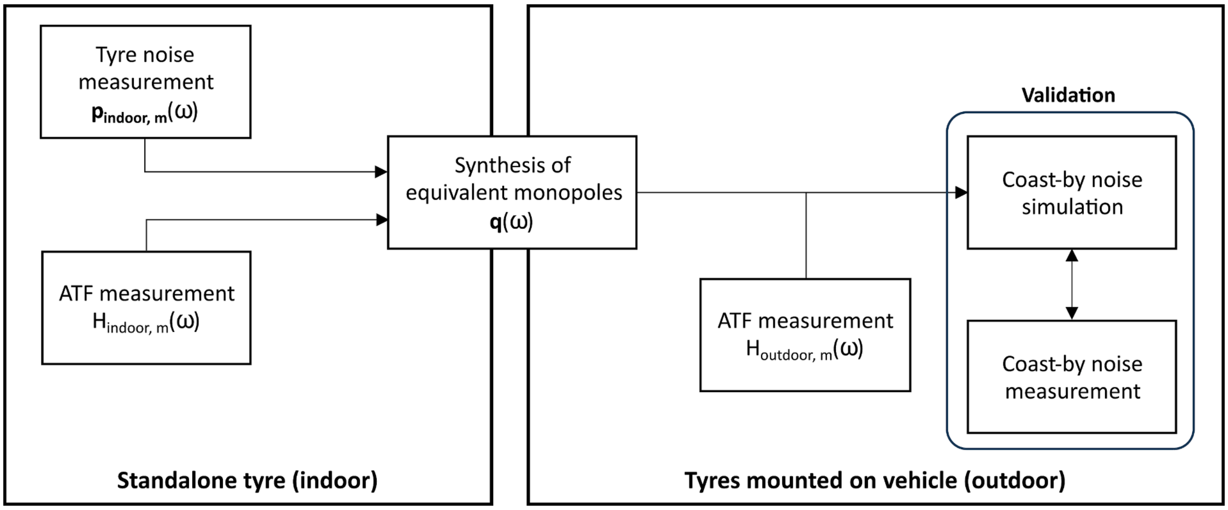

Fig. 1. Flowchart of the constant-speed coast-by simulation approach.

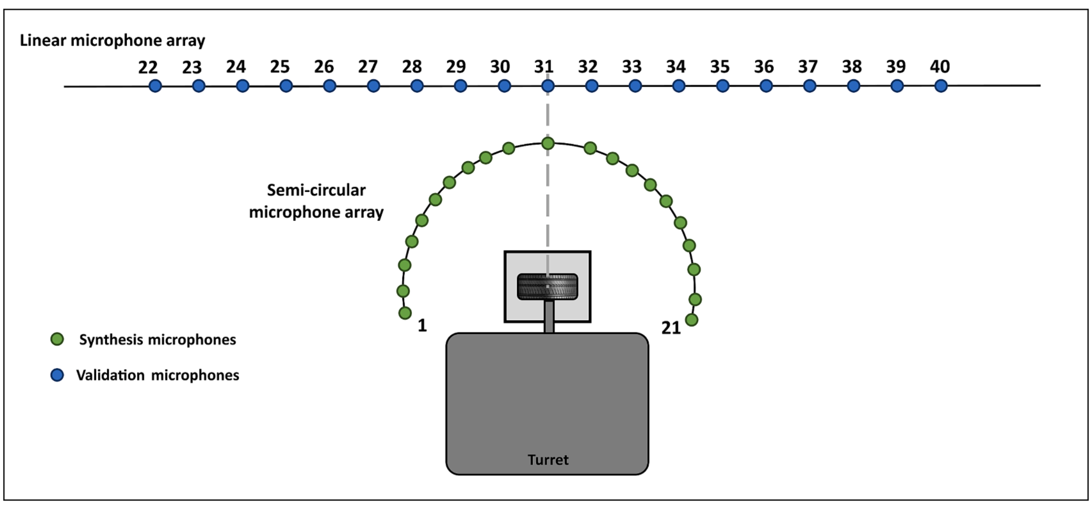

Fig. 2. Diagram of the indoor setup used for the identification of the equivalent sources. In green, the microphones used for the synthesis of the equivalent monopoles. In blue, the microphone used for validation purposes.

employed. A total of 21 microphones in a hemi-circular array configuration were used to identify the equivalent monopoles. A configuration of 14 complex equivalent sources surrounding the tyre footprint was adopted: 5 monopoles were placed both at the inlet and outlet of the tyre, and 4 in correspondence of the tyre side, towards the microphones. An additional set of 19 microphones on a linear array was employed for validation purposes only. The length, distance from the footprint and height of the microphones on the linear array are scaled with respect to the microphone setup prescribed by the ISO 362-3 standard [40] for indoor pass-by tests. Both sets of microphones were placed in the far-field region for the frequency range of interest (450 Hz–2820 Hz). Indeed, it is crucial that the monopoles accurately predict the sound field in the far-field region, as their intended application is for outdoor simulations.

Following the inverse approach, the identified equivalent monopoles were used to solve the direct problem to verify the accuracy of the predicted sound field ($H_{indoor} \bullet \boldsymbol{q}$) compared to the measured one. In Fig. 3, the application of the indoor synthesis methodology on a 225/45R17 tyre rolling at 80 km/h is shown. In particular, the Overall A-weighted Sound Pressure Levels (OASPL) obtained by solving the indoor problem are shown in comparison with experimental data both on the linear array and on the hemi-circular array, indicating good agreement.

Thus far, the methodology for obtaining the equivalent monopoles has been described. In indoor conditions, the equivalent sources and the microphones are fixed in space. Instead, for the development of the methodology for the outdoor simulation, it should be noted that these sources are moving as the vehicle travels along the test track while the microphones are stationary. In this case, the acoustic signals received by the microphones are affected by two main phenomena: the Doppler effect and time-varying propagation delays due to the finite speed of sound [27,34].

The Doppler effect refers to the frequency shift observed in the signal due to the relative motion between the sound source and the microphone. The frequency shift (Δf) due to the movement of the source relative to a stationary observer, considering air as the medium of wave propagation, can be expressed as follows [41]:

$$\Delta f = f_0 \frac{v_s \cos(\gamma)}{c - v_s \cos(\gamma)} \tag{1}$$

where f_0 is the emitted frequency, v_s is the velocity of the source relative to the observer, γ is the angle between the direction of the vehicle's motion and the line connecting the vehicle to the observer, and c is the speed of sound in air. As γ is time-dependent, the frequency shift varies as the vehicle travels along the track. In particular, Eq. (1) shows

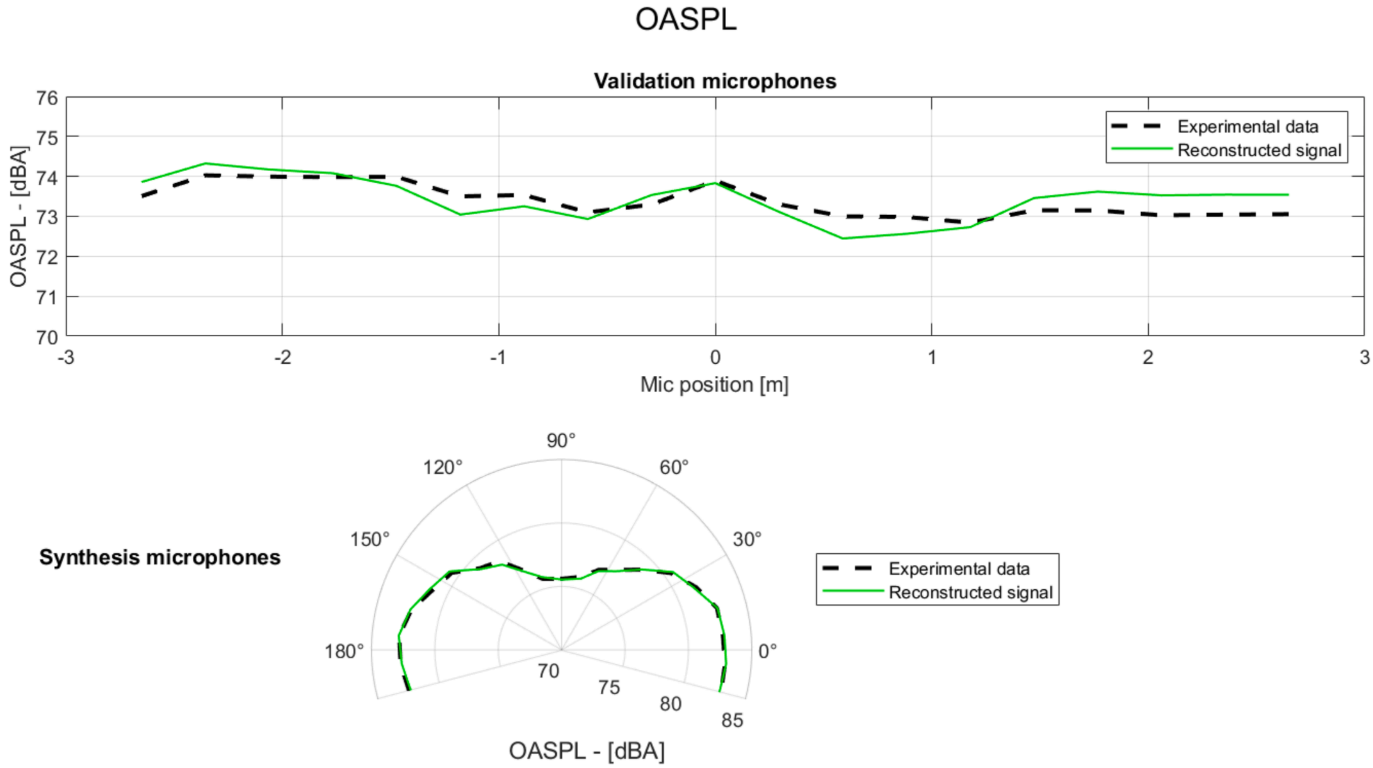

Fig. 3. Results of the synthesis procedure in indoor environment for a 225/45R17 tyre rolling at 80 km/h. The bottom panel shows the reconstructed signal (green) compared to experimental data (black) on the synthesis microphones, measured in OASPL. The top panel displays the reconstructed signal against experimental data on the validation microphones, also in terms of OASPL.

that as the vehicle approaches the microphone, the perceived frequency is higher than the emitted frequency, gradually matching the emitted frequency as the vehicle reaches the midpoint of the track ($\theta = 90^{\circ}$). While the vehicle moves away from the microphone, the perceived frequency decreases relative to the emitted frequency.

On the other hand, due to the distance between the source (vehicle) and the receiver and the finite speed of sound, a delay between the instant when the sound is emitted by the source and when it reaches the microphone is present. Moreover, the distance between the moving vehicle and the stationary microphone varies continuously while the vehicle advances. In conclusion, this distance introduces a varying time delay causing a difference between the source emission time (t_s) and receiver time (t_r), which is dependent on the changing distance between the source and the microphone [27,42].

In the proposed methodology, four tyres and the correspondent monopoles are considered at once. Therefore, multiple sources are employed, as identified during indoor conditions. The emission time is unique across all monopoles, as it is assumed that the sources begin emitting sound simultaneously. Instead, on the one hand a different distance between each corner and the receiver is present. On the other hand, focusing on the same corner, the monopoles also have different distances with respect to the receiver, due to their distinct locations around the tyre footprint. Therefore, a time delay ($\Delta t_i(t_s)$) characterizes each i-th source as there is a different distance between each source and receiver ($d_i(t_s)$). Finally, as the vehicle travels along the track, these distances further vary, and they are a function of the emission time. In conclusion, the relation between the emission and the receiver time ($t_{r,i}$) can be expressed as:

$$t_{r,i} = t_s + \Delta t_i(t_s) = t_s + \frac{d_i(t_s)}{c} \tag{2}$$

A methodology to include the effect of the relative motion between sources and receivers must be studied, taking into account that acoustic transfer function can be obtained only from static measurements (described in Section 3.2) or static acoustic transfer function simulations (out of the scope of this paper). For this reason, instead of simulating the vehicle's movement along the track, different positions occupied by the car in time were mapped by considering a linear array of receivers and a set of static sources, as shown in Fig. 4. The array and the set of sources must be in the same relative positions between the actual vehicle locations in the real test and the coast-by microphone.

In this processing, the receiver spacing dx is intrinsically bonded to the time discretization dt of the coast-by acoustic signal. The time discretization was computed as $dt = \frac{1}{f_{samp}} = \frac{1}{6 f_{max}}$, where $f_{max} = 2820\,Hz$ in the considered case study and a factor of 6 was chosen to avoid aliasing errors. Finally, considering a uniform rectilinear motion law of the vehicle, the space discretization of the receiver array can be calculated as $dx = v \bullet dt$. Considering a vehicle speed of 80 km/h and the proposed time discretization, receivers signal should be evaluated at approximately 1 mm intervals along the 20 m length of the track.

For correctly simulating the relative position between the coast-by microphone and the receiver, at each time instant t_s^j the acoustic transfer function $H_{outdoor}(x(t_s^j), \omega)$ between the static source and the receiver array must be considered. It is worth noticing that, as the vehicle's movement is simulated through different locations of the receiver along the track, the receiver travels in the opposite direction relative to the vehicle motion. Therefore, the outdoor acoustic transfer functions are evaluated at each time instant in $x\left(t_s^j\right)$, up to x_{max}, which is the maximum coordinate at which the acoustic transfer functions are known.

Once the acoustic transfer functions have been measured, the coast-by signal generated by a single source can be reconstructed. This is done by evaluating the product of the source strength spectra and the acoustic transfer functions, taken according to the relative position between source and receiver at each time instant. An inverse Fourier Transform is then applied to this product to obtain the time-domain signal. The

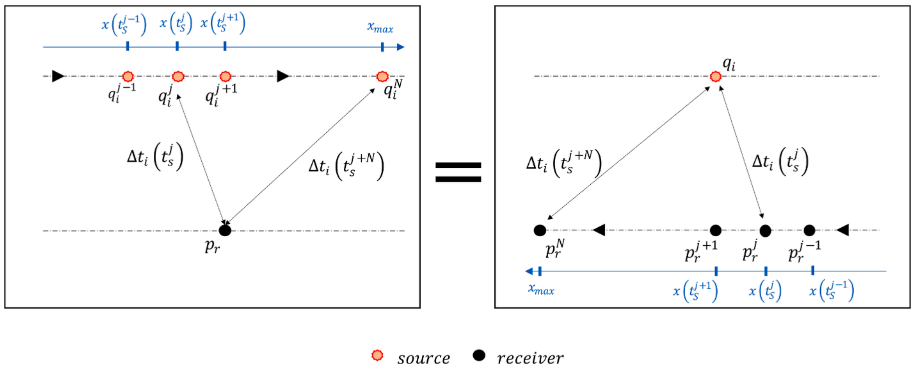

Fig. 4. Schematic representation of the coast-by simulation methodology. The sound pressure signal of a moving vehicle is simulated mapping at each time instant the relative position between a static vehicle and a linear array of microphones. The travelling direction of the source or the receiver is indicated through arrows on the direction line.

contribution of a single source $q_i(\omega)$ is given by:

$$p_i(t_r) = Re\left(\sum_{\omega} H_{outdoor,i}(x(t_s),\omega) \bullet q_i(\omega) \bullet e^{j\omega t_r}\right) \tag{3}$$

$H_{outdoor,i}$ intrinsically accounts for the time-delay associated with the finite speed of sound. For this reason, from Eq. (3) the term associated with the delay Δt_i can be made explicit as:

$$p_i(t_s + \Delta t_i(t_s)) = Re\left(\sum_{\omega} |H_{outdoor,i}(x(t_s),\omega)| \bullet e^{j(\varphi - \omega\Delta t_i(t_s))} \bullet q_i(\omega) \bullet e^{j\omega t_r}\right) \tag{4}$$

where φ is the phase component associated with the dynamic behaviour of the system, whereas the term $-\omega\Delta t_i(t_s)$ is related to the phase shift due to the delay Δt_i, which depends on both the source and the instant in which the sound pressure is evaluated. More details on the evaluation of the time-delay for each source will be given in Section 3.

Finally, the sound pressure level at the coast-by microphone $p_{CB}(t_r)$ can be computed by summing up the contributions of each source $p_i(t_r)$:

$$p_{CB}(t_r) = \sum_{i}^{N_s} p_i(t_r) \tag{5}$$

where N_s is the number of sources considered in the problem.

It is worth recalling that the processing applied in indoor conditions enabled the isolation of the deterministic contribution to the microphones' signals. As a result, the monopoles spectra also consisted of spectral components related to the tyre harmonics ω_{tread} and to the road roughness ω_{road}, and additional observations should be made. Firstly, when considering a simulation with a vehicle, four tyres are mounted. It was hypothesized that the equivalent monopoles shared the same amplitude among the four tyres, since in this work the same nominal load on the four tyres is guaranteed in outdoor conditions. However, it is not possible to assume that all four tyres are rolling with the same initial angular position. Indeed, even if tyres may be initially mounted with the same angular position, driving the vehicle inherently creates additional variations. For this reason, tyre harmonics between the four tyres should include phase delays due to random angular positions of the tread pattern. This additional phase delay is $e^{\frac{j\omega R\Delta\theta}{v}}$, where R is the tyre radius, $\Delta\theta$ is a randomly assumed angular shift and v is the vehicle speed. Moreover, further phase delays due to vehicle wheelbase and travelling speed should be taken into account by the road harmonics (roughness excitation). In fact, it can be considered that the rear wheel is affected by the same road roughness after a delay which is a function of both the distance between the front and rear axles and the vehicle speed. As a result, phase shifts are applied to the rear axle of the vehicle as $e^{\frac{j\omega L}{v}}$ to account for the delay due to running speed and wheelbase length L. Finally, an additional delay is introduced with the exponential $e^{j\omega\Delta T}$ where ΔT represents a random phase shift applied to the road excitation contribution at the left vehicle side with respect to the right one. A schematization of the applied delays for each vehicle corner is shown in Fig. 5. In order to adopt a statistical approach for studying the problem, multiple cases with the randomization of the phase delays defined above are considered, consequently obtaining 10 simulations of $p_{CB}(t_s)$.

As the final step, the exponentially weighted, time-averaged instantaneous Sound Pressure Level $SPL(t_r)$ can be obtained from the pressure for each load case:

$$SPL(t_r) = 10\log_{10}\left[\frac{1}{T}\int_{-\infty}^{t_r} p_{CB,A}^2(\tau)e^{\frac{\tau - t_r}{T}}d\tau\right] \tag{6}$$

with T being the decay time of the weighting function. According to the ISO 13325 standard, fast-weighting is employed, corresponding to T = 125 ms. Furthermore, for the overall SPL, an A-weighting filter is applied to $p_{CB}(t)$.

3. Outdoor experimental campaign

This section details the setup for outdoor testing for data collection in compliance with the ISO 13325 standard for coast-by noise evaluation. The measurements performed in this outdoor campaign are performed at Pirelli's outdoor test track in Vizzola Ticino (Italy). A detailed description follows, covering the experimental collection of acoustic transfer functions between the source and receivers, conducted on the noise track.

3.1. Coast-by measurements

For the assessment of tyres in terms of noise emission, the coast-by test is performed. The test involves evaluating tyre noise when mounted on the vehicle with the engine turned off (free rolling condition), in order to minimize disturbances caused by other noise sources. The coast-by test needs to be conducted in a prescribed area, characterized by a given geometry. Fig. 6 gives a visual representation of the test area for outdoor noise measurements.

Two microphones at the right- and left-hand side of the track are present for measuring sound pressure during the test. These microphones shall be located 1.2 ± 0.02 m above the test area surface and the distance from the centre line shall be 7.5 ± 0.05 m, The driver has to handle the vehicle in the test zone at a speed most possibly equal to 80 km/h, while keeping a straight trajectory as close as possible to the centre line of the drive lane. The noise track was featured with a photocell system that detects the vehicle's entry, ensuring its position is tracked during the test.

To guarantee the repeatability of these tests in different conditions, the test surface is compliant with the ISO 10844 prescriptions [43]. As

$$\begin{cases} q_{RL}(\omega_{tread}) = q(\omega_{tread}) \cdot e^{j\omega\frac{R\Delta\theta_{RL}}{v}} \\ q_{RL}(\omega_{road}) = q(\omega_{road}) \cdot e^{j\omega\Delta T} \cdot e^{j\omega\frac{L}{v}} \end{cases}$$

$$\begin{cases} q_{FL}(\omega_{tread}) = q(\omega_{tread}) \cdot e^{j\omega\frac{R\Delta\theta_{FL}}{v}} \\ q_{FL}(\omega_{road}) = q(\omega_{road}) \cdot e^{j\omega\Delta T} \end{cases}$$

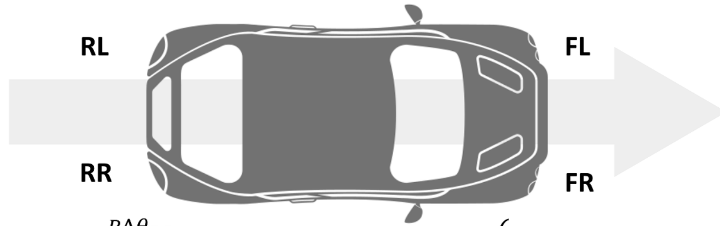

$$\begin{cases} q_{RR}(\omega_{tread}) = q(\omega_{tread}) \cdot e^{j\omega\frac{R\Delta\theta_{RR}}{v}} \\ q_{RR}(\omega_{road}) = q(\omega_{road}) \cdot e^{j\omega\frac{L}{v}} \end{cases}$$

$$\begin{cases} q_{FR}(\omega_{tread}) = q(\omega_{tread}) \cdot e^{j\omega\frac{R\Delta\theta_{FR}}{v}} \\ q_{FR}(\omega_{road}) = q(\omega_{road}) \end{cases}$$

Fig. 5. Delay formulation for each corner of the vehicle.

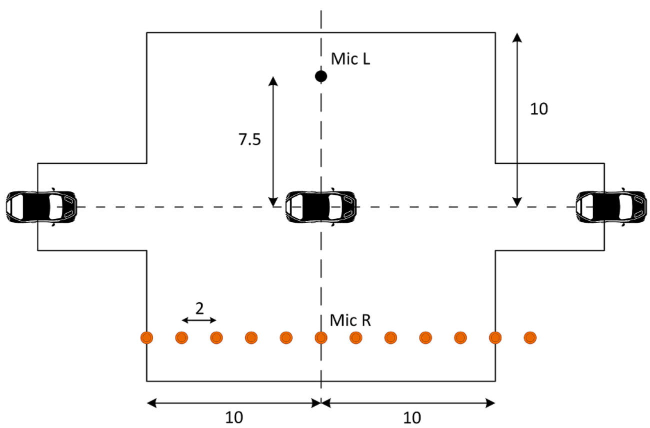

Fig. 6. Test area for outdoor noise measurements. In black, the microphone location for the coast-by noise measurement according to ISO 13325. In orange, the microphones' location for the acoustic transfer function measurement. Dimensions are specified in meters.

previously mentioned, given the importance of road asphalt characteristics, the equivalent sources in indoor conditions were identified starting from tyre rolling noise measurement on the road replica of the same outdoor noise track.

The coast-by tests were conducted on a BMW i3 electric vehicle to minimize external noise sources. Each of the four tyres with size 225/45R17 was loaded with 450 kg and inflated to a pressure of 2.2 bar, consistent with the indoor test conditions. Five test repetitions were performed at 80 km/h.

3.2. Outdoor source-receiver transfer function measurements

With the aim of performing the measurements of the acoustic transfer functions the vehicle is placed in the centre of the test track. The load on the four tyres is consistent with that in the coast-by measurement and indoor tests (450 kg). A microphone array of 12 microphones, evenly spaced 2 m apart on a single side of the track, was employed (Fig. 6). This setup was based on the assumption of symmetry of the acoustic source-receiver transfer functions between the left- and right-hand sides of the track. To carry out the methodology described in Section 2, the array is positioned at 7.5 m from the centre of the track on the right-hand side, at a height of 1.20 m.

The acoustic transfer functions were determined experimentally using a mid-high frequency Qsource (Q-MHF) by Siemens. The Qsource is an omnidirectional acoustic source that incorporates a volume acceleration probe. The measurement system allowed for the synchronous acquisition of the volume acceleration at the Qsource and the sound pressures at the receivers. In particular, a broadband white noise was chosen to drive the Qsource. The matrix $H_{outdoor}$ representing the measured acoustic transfer functions was calculated by treating the signal recorded by the omnidirectional acoustic sensor as input and the sound pressures measured at the receiver as outputs. These transfer functions are evaluated using the H_1 estimator, dividing the signal in 1 s windows for averaging. Each of them is expressed in $Pa/m^3/s^2$ representing sound pressure levels (Pa) for a single monopole activation with a unitary volume acceleration (m^3/s^2).

The nozzle of the omnidirectional source was positioned at the monopoles' locations around the tyre footprint, for the measurement of the source-receiver transfer functions for a monopole at a time. It is important to note that, since the acoustic transfer functions were measured with the tyres mounted on the vehicle and directly on the test track, the influence of both the vehicle and its associated acoustic effects, as well as those of the track pavement, are inherently taken into account. The setup used during the experimental campaign is shown in Fig. 7: in Fig. 7a an example of the placement of the acoustic source in correspondence of a monopole in the tyre inlet is shown, while in Fig. 7b the test track and the microphones located on the side of the track are shown, including the placement of the vehicle at the centre of the noise track. The measurements for all the corners of the vehicle are performed in the same day, without moving either the vehicle or the microphones, so that no errors due to repositioning of the car or the microphones could affect the results.

As previously mentioned, a configuration of 14 complex equivalent sources was adopted in indoor conditions. In outdoor conditions, the same layout was applied to perform the coast-by prediction. Specifically, the acoustic transfer functions of the monopoles surrounding the tyres' footprints were measured for both tyres on the right side of the vehicle, facing the microphone array. In contrast, preliminary analyses on the acoustic transfer functions of the tyres opposite to the array of receivers have shown that only the inlet monopoles of the front left tyre and the outlet ones of the rear left tyre have a non-negligible contribution to the receiver array. Indeed, it is expected that the inlet of the front left tyre will contribute as the vehicle enters the track, while the outlet of the rear left tyre will contribute as the vehicle exits the track. The other locations have a negligible contribution due to the masking effects given by the vehicle and the other tyres. This enabled a reduction of the total time dedicated to the experimental campaign for the measurement of the acoustic transfer functions. A total of 38 monopoles were considered, with 28 positioned on the tyres on the same side as the microphone array, 14 on the front right and 14 on the rear right tyres. Additionally, 5 are placed on the front left inlet, and 5 on the rear left outlet. A

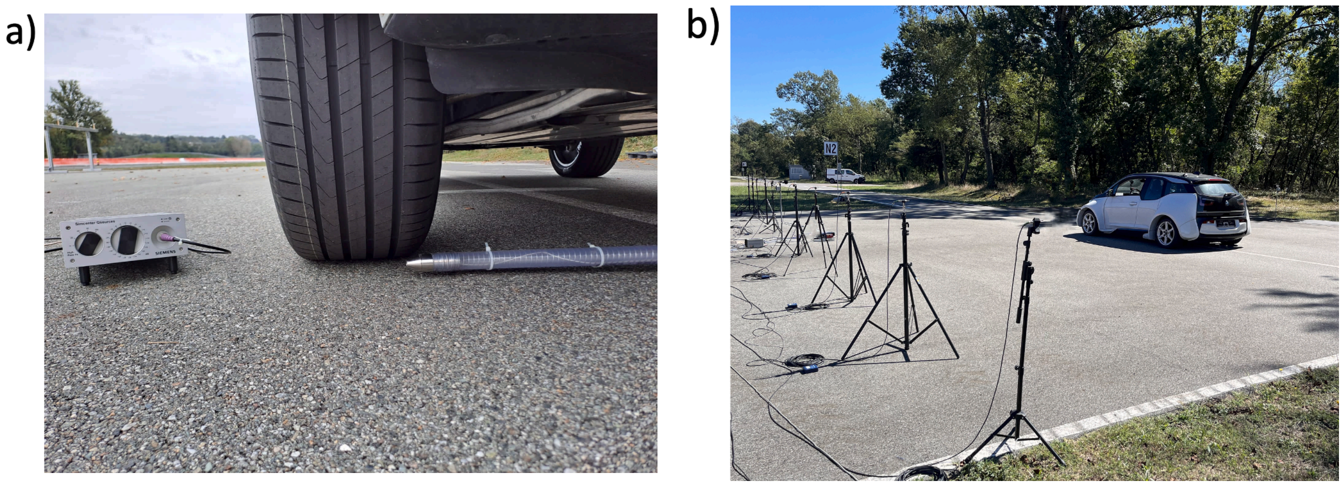

Fig. 7. a) Qsource positioned in correspondence of the tyre's inlet. b) Noise track and microphone layout for the measurement of the acoustic transfer functions.

schematization of the placement of the monopoles is reported in Fig. 8.

As mentioned in Section 2, a spacing of around 1 mm between the microphones would be required to meet the imposed constraints. However, as the acoustic transfer functions were experimentally measured in this study, the use of around 20,000 microphones was not feasible. For this reason, once the acoustic transfer functions were obtained with a coarser spatial discretization (2 m), a strategy to obtain the acoustic transfer functions at additional spatial positions was implemented. Regarding the absolute values of the acoustic transfer functions, the magnitude was interpolated in the spatial domain at each frequency. As for the phases, the delay due to the sound propagation time through air, which depends on the source-receiver distance, must be considered. To this end, a dedicated post processing of the signals was conducted to estimate the source-dependent time delay Δt_i at the known microphone locations, that accounts for the time-varying propagation delay due to the finite speed of sound. Once determined, the delays at these positions were interpolated to estimate their values at unknown locations, achieving the desired spatial discretization. The procedure was repeated for each monopole source. These computed delays serve two purposes: first, to estimate the phase of the acoustic transfer functions associated with the $e^{-j\omega\Delta t_i(t_s)}$ term of Eq. (4), and second, to accurately map the receiver time t_r during the coast-by prediction. Fig. 9 illustrates the delay for a monopole located at the inlet of each front tyre and at the outlet of each rear tyre, providing a visualization of the time-varying delay specific to each source and reflecting the changing distance between source and receiver as the vehicle travels along the track. As expected, the delay was shorter where the distance between the microphones and the source was minimal and increased with greater distances. Indeed, the smallest delays were observed at the corners closer to the microphone array. The minimum measured delay aligned with the calculated one, assuming a sound speed of 343 m/s and considering a 6.7 m distance between the monopole and the receiver, which accounts for the vehicle track width.

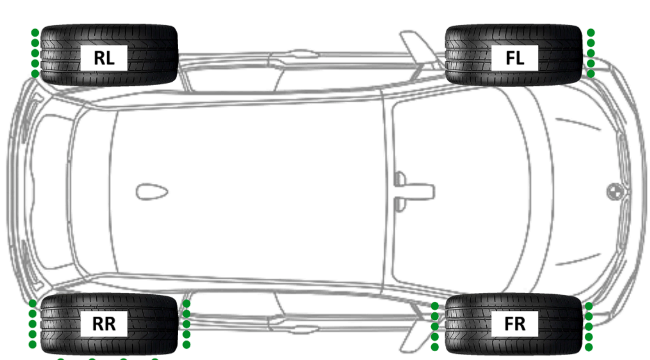

Fig. 8. Schematization of the monopole placement for the evaluation of the acoustic transfer functions and the coast-by noise prediction.

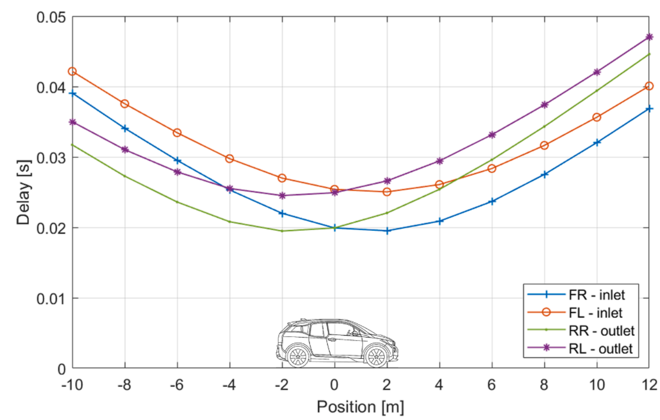

Fig. 9. Delay between the emitter time and receivers time for the case of a monopole located at the front right, front left, rear right and rear left tyres.

4. Coast-by prediction

This section presents the results of the methodology used for the coast-by prediction and its comparison with experimental data. It is possible to represent OASPL as function of the vehicle location along the track and compare it with experimental data, obtained according to Eq. (6). The results are presented for the considered 225/45R17 tyre at 80 km/h in Fig. 10. In particular, the graph illustrates in dark grey the variability in terms of OASPL for the experimental data across the 5 test repetitions. For the coast-by prediction, 10 randomizations of the phases corresponding to the delays in the term $q(\omega)$ represented in Fig. 5 were considered, resulting in a range of values for each position represented by a green envelope in the graph. The solid line in both cases represent the average value.

Regarding the OASPL levels, the comparison between the experimental coast-by data and the prediction reveals some differences both in the trend along the track and in the absolute levels, with errors below 2.5 dB as the vehicle travels along the track. The observed discrepancies may be attributed to different aspects. It is important to emphasize the distinct operating conditions of the tyre during indoor tests, where the equivalent monopoles were synthesized, compared to outdoor tests: during indoor tests the tyre is loaded against a curved drum surface,

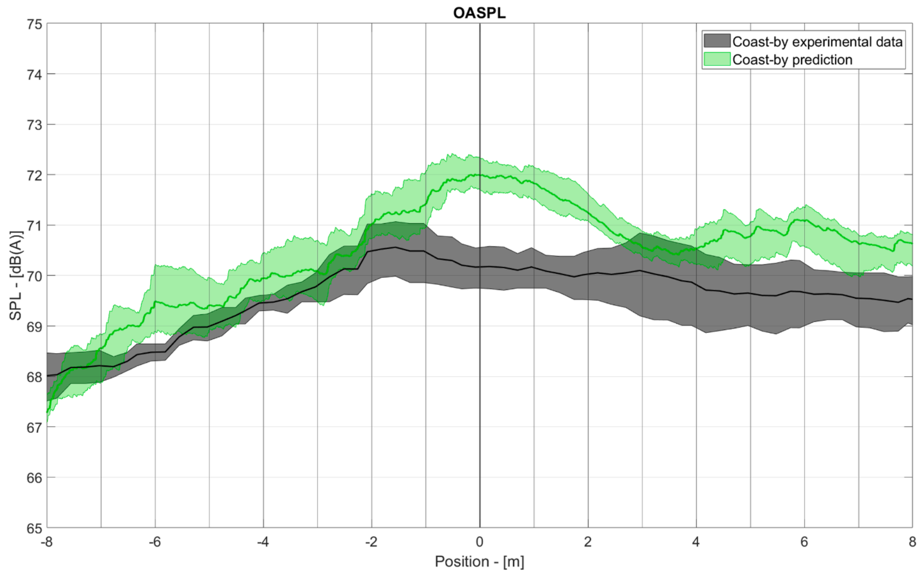

Fig. 10. Comparison of the simulated OASPL (green) and measured OASPL (black). The shaded areas indicate the range of maximum and minimum levels recorded accounting for the different test repetitions.

whereas outdoor tests involve contact with a flat track. This difference alters tyre deformation and contact pressure distribution, which in turn affects the mechanisms of vibration generation, noise emission and its amplification. Differences between laboratory and CPX measurements are also found in [44]. Future research could explore this topic further, focusing on the influence of flat versus drum boundary conditions on the acoustic behaviour of the rolling tyre. Additionally, differences in construction materials may lead to variations in surface roughness, which can consequently affect the acoustic response. Lastly, measurement uncertainties related to the positioning of the Qsource during the acquisition of the acoustic source-receiver transfer functions could also play a role.

As an alternative visualization, it is also possible to visualize the predicted sound pressure levels trend in frequency and space at the coast-by microphone. The spectrogram has been obtained by averaging the 10 repetitions considered by randomising the phases correspondent to the tyre and road roughness excitations. The result for the considered test case is shown in Fig. 11.

This visualization highlights that the predominant frequencies in the simulation results correspond to the 1000–1250 one-third octave bands region. The elevated levels in this frequency range can be attributed to the higher source strengths of the monopoles identified in the indoor environment. Additionally, the representation reveals the presence of the Doppler effect, which is particularly noticeable in the higher amplitude harmonics. To better illustrate its effect, the graph includes lines indicating the frequency shift, calculated according to Eq. (1), for f_0 values of 900, 1000 and 1100 Hz. The analysis shows that the typical “s” shaped trend with a perceived frequency higher than the nominal one (f_0) at the 0 m position during the approaching phase, and lower during the receding phase. The comparison with experimental data, instead,

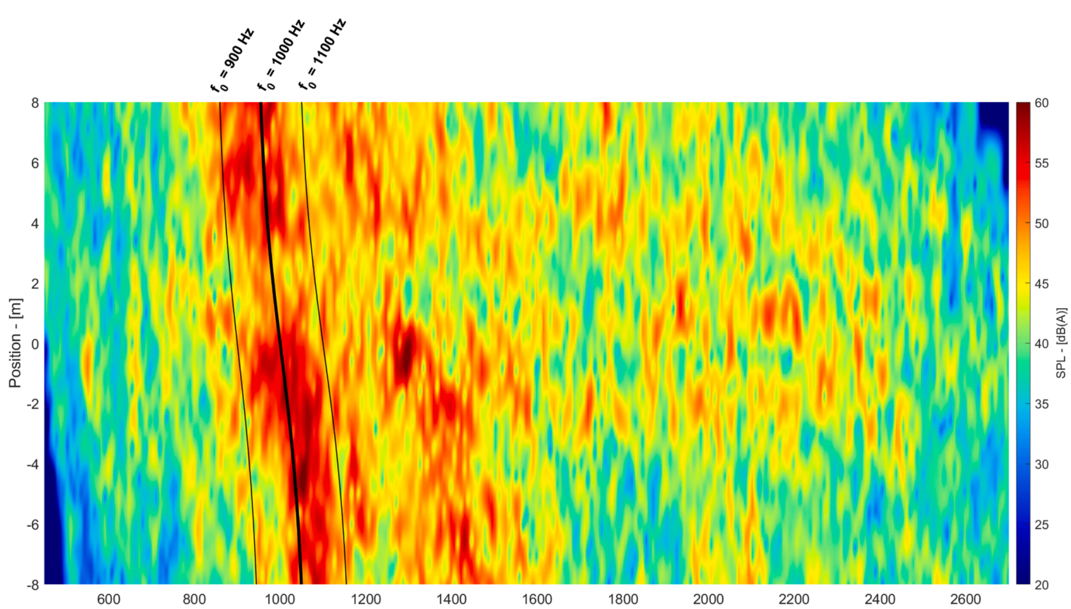

Fig. 11. Average spectrogram obtained from the coast-by simulations. In black lines, the trend in frequency due to the Doppler effect considering the emitter frequency f_0 at 900, 1000 and 1100 Hz at the 0 m location.

shows differences in terms of the frequency content.

The comparison of the one-third octave band frequency content between the coast-by simulation and the experimental data reveals some differences. Fig. 12a shows the one-third octave band comparison between the predicted coast-by results and the experimental data at the position of maximum OASPL. In general, the simulation yields higher levels, consistent with the OASPL trends. Additionally, the simulated data reach their maximum levels at the one-third octave band centered at 1000 Hz (Fig. 12b), whereas the experimental measurements show higher levels at lower frequencies, around 800 Hz (Fig. 12c). This discrepancy can be attributed to the differing contact conditions in indoor (drum) and outdoor (flat-road) tests. In particular, this frequency range is influenced by acoustic amplifications known as pipe resonances [11,45,46]. Under outdoor conditions, a longer contact patch is expected. Since the pipe resonance frequency decreases with increasing groove length, the longer contact patch in outdoor tests results in lower pipe resonance frequencies, which may help explain the enhanced low-frequency content observed in the experimental data. Moreover, a possible overlap between the pipe resonances and the tread pitch frequency may contribute to the high SPL levels observed in certain frequency bands.

The developed methodology can also be adopted for more detailed analyses. For instance, it allows for the separation of each corner's contribution to the total sound pressure levels. This analysis is carried out by activating only the monopoles associated with the considered corner and then performing the coast-by prediction. The results for the test case considered are presented in Fig. 13, showing the average values of individual contributions to the coast-by prediction at the right microphone. This contribution plot shows that the front right corner initially has the highest contribution as the vehicle enters the track. However, its contribution is exceeded by that of the rear right corner. The greater contributions from the right corners compared to the left ones are expected due to their proximity to the predicted microphone. For what concerns the left-hand side corner, the front left contributes more significantly at negative positions, corresponding to the vehicle entering the track. This is due to the fact that in this region it is less masked by the vehicle body and the other tyres. Similarly, the rear left corner shows higher contribution as the vehicle exits the track, where it is directly exposed to the microphone. These trends align with the expected behaviour based on the geometrical arrangement and acoustic propagation characteristics.

5. Conclusions

This paper presented a methodology for the outdoor coast-by prediction. The approach involved the use of equivalent sources identified through indoor testing and acoustic source-receiver transfer functions measured in outdoor conditions for the prediction of the sound pressure levels at the coast-by microphone. The process begins with the identification of a set of equivalent monopoles by means of indoor tests by combining experimentally measured transfer functions and sound pressure levels measured at specific far-field microphone positions. The tests for the synthesis procedure are carried out inside a semi-anechoic chamber and considering a standalone tyre on drum equipped with a road replica. The equivalent sources were synthesised based on the spectral components related to the tyre harmonics and to the road roughness. Next, the acoustic transfer functions in outdoor conditions were experimentally measured, accounting for the presence of the vehicle and the deformed tyre geometry. A methodology for their interpolation at unknown locations is also described.

A frequency-domain methodology has been developed to perform the outdoor coast-by prediction. The proposed approach accounts for both the Doppler effect and time-varying propagation delays due to the finite speed of sound, caused the physical phenomena associated with measuring moving acoustic sources through a stationary microphone. Furthermore, a statistical approach for studying the problem has been considered, simulating multiple passages of the vehicle in front of the microphone by randomizing the phase delays associated with the contributions of the tread and the road. The results showed that the prediction approximates the trend of the sound field while the vehicle travels along the track, with an overestimation of 2.5 dB of the sound pressure levels evaluated at the coast-by microphones. The discrepancies between the predicted and measured data may be due to variations in the contact patch conditions, such as the flat surface in outdoor tests compared to the drum surface used during indoor experiments, where the monopoles are identified. Furthermore, although the indoor track replicates the outdoor asphalt, differences in materials may still produce variations in acoustic behavior.

Further developments of the approach may involve different areas of investigation. Firstly, examining the differences between flat and drum conditions could provide insights into the correlation between experimental measurements and prediction. Moreover, the approach could be extended to use numerically evaluated acoustic transfer functions, eliminating the need for a dedicated experimental campaign for their

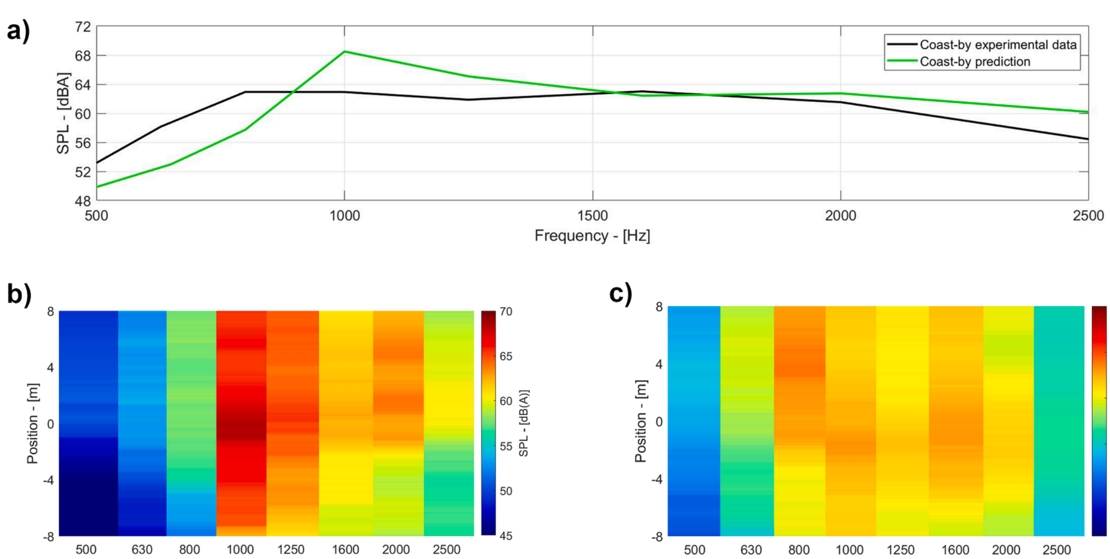

Fig. 12. a) Comparison of the one-third octave band levels between the predicted (green) and experimental (black) data at the position of maximum oaspl. b) One-third octave band averaged spectrogram from the coast-by simulation. c) One-third octave band averaged spectrogram from the coast-by experimental tests.

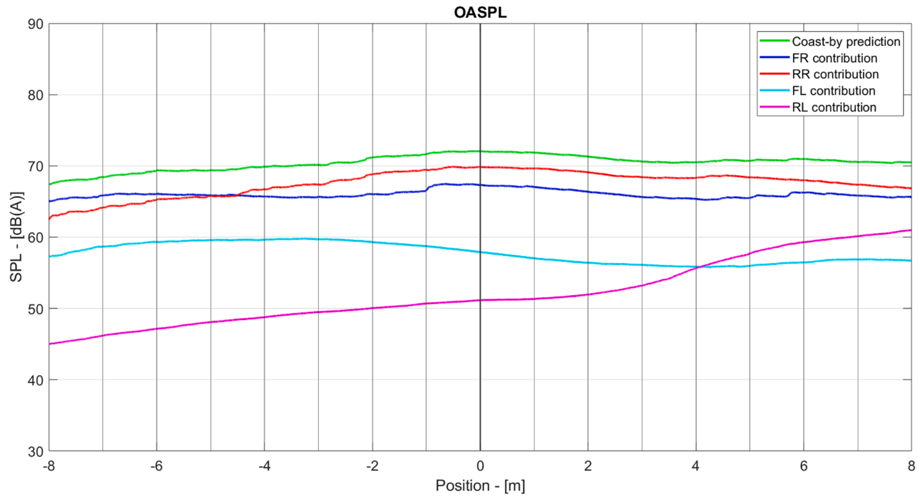

Fig. 13. Contribution of each corner to the OASPL.

measurement both in indoor and outdoor conditions. Finally, the investigation could be expanded to include other tyres in order to assess the methodology ability to rank tyres based on their noise emission.

CRediT authorship contribution statement

Samanta Dallasta: Writing – original draft, Validation, Methodology, Investigation, Conceptualization. **Luca Rapino:** Writing – review & editing, Supervision, Methodology, Conceptualization. **Francesco Ripamonti:** Writing – review & editing, Supervision, Conceptualization. **Simone Baro:** Writing – review & editing, Supervision, Conceptualization. **Roberto Corradi:** Writing – review & editing, Supervision, Project administration, Conceptualization.

Declaration of competing interest

The authors declare that they have no known competing financial interests or personal relationships that could have appeared to influence the work reported in this paper.

Acknowledgements

This study is part of the AirBorne Exterior Noise (ABEN) research project, carried out in the framework of the Joint Labs cooperation agreement between Politecnico di Milano and Pirelli. The authors gratefully acknowledge Pirelli for providing the support and data necessary for this work.

Data availability

The data that has been used is confidential.

References

[1] Environment ECD-G for, Kantor E, Klebba M, Richer C, Kubota U, Zeisl Y, et al. Assessment of potential health benefits of noise abatement measures in the EU – Phenomena project. Publications Office; 2021. https://doi.org/doi/10.2779/24566.
[2] Khomenko S, Cirach M, Barrera-Gómez J, Pereira-Barboza E, Iungman T, Mueller N, et al. Impact of road traffic noise on annoyance and preventable mortality in European cities: a health impact assessment. Environ Int 2022;162:107160. https://doi.org/10.1016/J.ENVINT.2022.107160.
[3] World Health Organization. Regional Office for Europe. Environmental noise guidelines for the European Region n.d.
[4] Bernhard R, Wayson R. An introduction to tire/pavement noise of asphalt pavement. Quiet and Durable Highways: Institute of Safe; 2005.
[5] Sandberg U, Ejsmont JA. Tyre/Road Noise Reference Book. vol. 1. 2002.
[6] ETRMA. Tyre & Road traffic noise Where we should look for road traffic noise improvements. 2021.
[7] EU. Regulation (EU) 2020/740 of the European Parliament and of the Council of 25 May 2020 on the labelling of tyres with respect to fuel efficiency and other parameters, amending Regulation (EU) 2017/1369 and repealing Regulation (EC) No 1222/2009 2020.
[8] Berge T, Mioduszewski P, Hałucha M, Bohatkiewicz J. ISO test track influence on the EU tyre label noise value. Appl Acoust 2025;228:110315. https://doi.org/10.1016/J.APACOUST.2024.110315.
[9] Ling S, Yu F, Sun D, Sun G, Xu L. A comprehensive review of tire-pavement noise: Generation mechanism, measurement methods, and quiet asphalt pavement. J Clean Prod 2021;287. https://doi.org/10.1016/j.jclepro.2020.125056.
[10] Bernhard RJ, Sandberg U. Tire-pavement noise: where does it come from? TR News 2005.
[11] Li T. A review on physical mechanisms of tire-pavement interaction noise. SAE Int J Veh Dyn Stab NVH 2019;3. https://doi.org/10.4271/10-03-02-0007.
[12] Kropp W, Bécot F-X, Barrelet S. On the sound radiation from tyres. Acust 2000;86:769–79.
[13] Winroth J, Kropp W, Hoever C, Beckenbauer T, Männel M. Investigating generation mechanisms of tyre/road noise by speed exponent analysis. Appl Acoust 2017;115:101–8. https://doi.org/10.1016/j.apacoust.2016.08.027.
[14] Wang X. Automotive tire noise and vibrations: analysis. Measure Simul 2020. https://doi.org/10.1016/B978-0-12-818409-7.00016-7.
[15] Fry J, Jennings P. Using multi-layer perceptrons to predict vehicle pass-by noise. Neural Comput Applic 2003;11. https://doi.org/10.1007/s00521-003-0354-3.
[16] Redel-Macías MD, Fernández-Navarro F, Antonio Gutiérrez P, Cubero-Atienza AJ, Hervás-Martínez C. Ensembles of evolutionary product unit or RBF neural networks for the identification of sound for pass-by noise test in vehicles. Neurocomputing 2013;109:56–65. https://doi.org/10.1016/J.NEUCOM.2012.03.022.
[17] Fry J, Jennings P, Taylor N, Jackson P. Vehicle drive-by noise prediction: a neural networks approach. SAE Technical Papers 1999. https://doi.org/10.4271/1999-01-1740.
[18] Beckenbauer T, Klein P, Hamet J-F, Kropp W. Tyre/road noise prediction: a comparison between the SPERoN and HyRoNE models - Part 1. Proc Eur Conf Noise Control 2008:2933–8.
[19] Klein P, Beckenbauer T, Hamet JF, Kropp W. Tyre/road noise prediction: a comparison between the SPERoN and HyRoNE models - Part 2. Proc Eur Conf Noise Control 2008. https://doi.org/10.1121/1.2934049.
[20] Ryu Y, Lange S. The Design and Validation of Simulated Indoor Passby Noise Measurement System. SAE Technical Papers, vol. 2007- January, 2007. https://doi.org/10.4271/2007-26-033.
[21] Alkmim M, Cuenca J, de Ryck L, Janssens K, Kournoutos N, Papaioannou A, et al. A semi-circular microphone array configuration for indoor pass-by noise sound synthesis. Proceedings of 2020 International Congress on Noise Control Engineering, INTER-NOISE 2020, 2020.
[22] Ryu Y. The optimum array design for the indoor simulated pass-by noise measurement system. 12th International Congress on Sound and Vibration 2005, ICSV 2005, vol. 5, 2005.
[23] Genuit K, Guidati S, Sottek R. Progresses in pass-by simulation techniques. SAE Technical Papers 2005. https://doi.org/10.4271/2005-01-2262.
[24] Clar-Garcia D, Velasco-Sanchez E, Sanchez-Lozano M, Campello-Vicente H. An alternative Drum test method to UNECE Regulation 117 for measuring tyre/road noise under laboratory controlled conditions. Appl Acoust 2019;151. https://doi.org/10.1016/j.apacoust.2019.03.005.
[25] Verheij JW. Inverse and Reciprocity Methods for Machinery Noise Source Characterization and Sound Path Quantification Part 1: sources. Int J Acoust Vibr 1997:2. https://doi.org/10.20855/ijav.1997.2.107.
[26] Vansant K, Bériot H, Bertolini C, Miccoli G. An update and comparative study of acoustic modeling and solver technologies in view of pass-by noise simulation. SAE Int J Engines 2014;7. https://doi.org/10.4271/2014-01-2073.

[27] Huijssen J, Hallez R, Pluymers B, Desmet W. A synthesis procedure for pass-by noise of automotive vehicles employing numerically evaluated source-receiver transfer functions. J Sound Vib 2013;332. https://doi.org/10.1016/j.jsv.2013.01.042.
[28] Calloni M, Musser C, Castel A, Mejdi A, Medeiros A. A Pass-By Noise Prediction Method Based on Source-Path-Receiver Approach Combining Simulation and Test Data. SAE Technical Papers, vol. 2019- January, 2019. https://doi.org/10.4271/2019-26-0188.
[29] Danti M, Biasiolo M, Amodeo D, Di Nenno G. A hybrid approach for the assessment of paths in pass-by Maneuver. SAE Technical Papers 2020. https://doi.org/10.4271/2020-01-1550.
[30] Huijssen J, Fiala P, Hallez R, Desmet W. Simulation of pass-by noise of automotive vehicles in the mid-frequency range using Fast Multipole BEM. Proceedings of ISMA 2010 - International Conference on Noise and Vibration Engineering, including USD, 2010. 2010.
[31] Eisele G, Alt N, Pichot F. Vehicle exterior noise simulation. 13th International Congress on Sound and Vibration 2006, ICSV 2006, vol. 2, 2006. https://doi.org/10.1007/bf03224885.
[32] Chen K, Jiang S-W, Zhang X-D. Analysis of noise source contribution in vehicle based on operational transfer path analysis method. J Shenyang Univ Technol 2021;43:652–61. https://doi.org/10.7688/j.issn.1000-1646.2021.06.10.
[33] Liu C, Zhang X, Zhang Y. An improved time-domain equivalent source method for accurate indoor simulation of pass-by noise. J Vib Acoust 2023;145. https://doi.org/10.1115/1.4056195.
[34] Kim B-K, Yoo S, Kim H, Zwanzig K. Prediction of vehicle pass-by noise using indoor measurements. SAE Technical Papers 2001. https://doi.org/10.4271/2001-01-1563.
[35] Chen J, Liu C, Zhang XZ, Bin ZY, Li JZ. An approach for indoor prediction of the pass-by noise of a vehicle based on the time-domain equivalent source method. Mech Syst Sig Process 2021;146:107037. https://doi.org/10.1016/J.YMSSP.2020.107037.
[36] Rapino L, Ripamonti F, Dallasta S, Baro S, Corradi R. Synthesis of equivalent sources for tyre/road noise simulation and analysis of the vehicle influence on sound propagation. Appl Acoust 2024;216:109751. https://doi.org/10.1016/J.APACOUST.2023.109751.
[37] Dallasta S, Rapino L, Ripamonti F, Corradi R, Baro S. Synthesis of equivalent sources from indoor measurements for tyre/road noise simulation. Proceedings of the International Congress on Sound and Vibration. 2024.
[38] Dallasta S, Rapino L, Ripamonti F, Baro S, Corradi R. Accounting for the vehicle influence on tyre noise through acoustic simulation based on equivalent monopole sources. Inter-Noise and Noise-Con Congress and Conference Proceedings 2024; 270:9045–51. https://doi.org/10.3397/IN_2024_4177.
[39] Dallasta S, Rapino L, Ripamonti F, Baro S, Corradi R. Tyre/road noise modelling through equivalent monopoles: source strengths identification based on experimental acoustic transfer functions. Appl Acoust 2025;236. https://doi.org/10.1016/j.apacoust.2025.110719.
[40] ISO 362-3:2022 - Acoustics - Measurement of noise emitted by accelerating road vehicles - Engineering method. Part 3: Indoor testing M and N categories 2022.
[41] Pierce AD. Acoustics: an introduction to its physical principles and applications. Third Edition 2019. https://doi.org/10.1007/978-3-030-11214-1.
[42] Vancauter R. A doppler correction procedure for exterior pass-by noise testing. SAE Technical Papers 1997. https://doi.org/10.4271/971987.
[43] International Standardization Organization (ISO). ISO 10844:2021 Acoustics — Specification of test tracks for measuring sound emitted by road vehicles and their tyres n.d.
[44] Wieczko-Zurek B, Ejsmont J, Ronowski G, Taryma S. Comparison of road and laboratory measurements of tyre/road noise. INTERNOISE 2014 - 43rd International Congress on Noise Control Engineering: Improving the World Through Noise Control, 2014.
[45] Rapino L, Ripamonti F, Baro S, Corradi R. Numerical Analysis of the Tread Grooves' Acoustic Resonances for the Investigation of Tire Noise. J Vib Acoust 2024;146. https://doi.org/10.1115/1.4066313.
[46] Pinay J, Saito Y, Mignot C, Gauterin F. Understanding the contribution of groove resonance to tire-road noise on different surfaces under various operating conditions. Acta Acust 2020;4. https://doi.org/10.1051/aacus/2020004.